

Ultra-reliable Communication over Vulnerable Optical Networks via Lightpath Diversity: Receiver Architectures and Performance

Yonggang Wen, *Student Member, IEEE* and Vincent W. S. Chan, *Fellow, IEEE*

Laboratory for Information and Decision Systems
Massachusetts Institute of Technology
Cambridge, MA, USA 02139
ewyg@mit.edu and chan@mit.edu

Abstract—In this paper we develop a class of structured receivers for a lightpath diversity scheme, which was introduced to provide ultra-reliable communication with low delay in vulnerable all-optical networks. We explore the trade-off between implementation complexity and error probability to achieve optimum and near-optimum performance within a class of structured receivers. Using a Doubly-Stochastic Point Process model, we develop receiver architectures for both the optimal receiver with respect to error performance, and the equal-gain-combining receiver with sub-optimum error performance but simpler receiver architecture. Closed-form error bounds for both receivers are obtained and compared with the ‘Genie-aided’ limit of the lightpath diversity transmission scheme. The comparison shows that the error performance of both receivers approaches the ‘Genie-aided’ limit when the signal is strong. Numerical results also demonstrate that additional power over what is required for the optimum receiver is needed to be transmitted in order for the equal-gain-combining receiver to achieve the same target error probability, and the power penalty decreases with decreasing noise level. These results suggest that the simpler equal-gain-combining receiver provides similar performance as the optimal receiver in the high signal-to-noise ratio (SNR) regime, but the optimal receiver should be used in the low SNR regime for significantly better performance.

I. INTRODUCTION

When deployed, all-optical networks [1][2], will trigger an architectural revolution for future broadband networks by eliminating all optical-to-electrical conversions along the lightpath. Originally proposed to exploit the huge bandwidth within the low attenuation transmission window of optical fibers to meet the exponential growth of traffic demand, optical networks have been evolved to provide other highly desirable features, such as wavelength switching, dynamic reconfiguration and improved reliability. These enhanced features can support highly reliable services that can transport, for instance, aircraft control signals between cockpit and control surfaces over lightweight all-optical networks.

However, as in other networks, all-optical networks are also vulnerable to component failures, such as fiber cut and node hardware failure. To counteract these failures, one prevailing method, the protection-switching mechanism [3][4], is to locate these failures and restore the connection via either shared or dedicated backup links or lightpaths. Unfortunately, the protection-switching mechanism can induce a rather long delay (e.g., 50-ms restoration time, a Synchronous Optical Network (SONET) standard [5]). The high delay during restoration makes it inappropriate for transporting critical messages, which may have tight delivery deadline (~1-ms) faster than the speed at which most optical components can switch, over all-optical networks.

In order to achieve ultra-reliable communication with low delay in all-optical networks, we have proposed using multiple link-disjointed lightpaths [6] to provide end-to-end reliable data delivery in the presence of failures. The mechanism is illustrated in Fig. 1. For each channel symbol, the modulated lightwave is split and sent through multiple independent lightpaths. At the receiver, received optical signals are either combined optically before detection, or individually detected and electrically combined for symbol-by-symbol decisions.

The advantages of the proposed reliable transmission scheme, which is based on spatial diversity via multiple disjoint lightpaths belonging to different shared-risk groups, are at least two-fold. First, because the entire mechanism is implemented at the Physical Layer and reaction time is within a single symbol interval, it provides a much faster response to failures than protocols that provide end-to-end reliability at higher layers, such as the Transmission Control Protocol (TCP) at the Transport Layer. Second, as shown in [6], the symbol error probability of light-diversity transmission is significantly lower than that of single-lightpath transmission in medium and high signal-to-noise ratio (SNR) regimes. In particular, for a source-destination pair connected by M lightpaths, the symbol error probability in the high SNR regime is asymptotically f^M ,

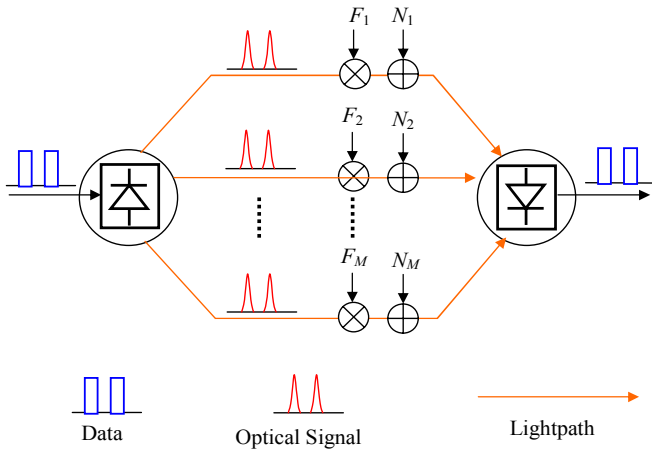


Fig. 1. The lightpath diversity transmission scheme.

where f is the individual lightpath failure probability. This is the asymptotic reliability limit of the multiple-lightpath transmission scheme. By choosing the number of lightpaths used, this limit can be made arbitrarily small compared to the asymptotic symbol error probability of using a single lightpath between the source-destination pair.

We have characterized the lightpath diversity architecture using a Doubly-Stochastic Point Process model and an idealized Genie-aided receiver in [6]. Using the derived symbol error probability, we have also optimized the system performance under different objective functions by choosing an optimum number of lightpaths. These performance limits, called the Genie-aided limits, can serve as a benchmark for the design of more practical receivers. In this paper, we develop a class of easily implementable structured receivers and compare their performance to that of the Genie-aided receiver.

This paper is organized as follows. In Section II, a class of structured receivers is proposed, and the error-complexity trade-off is discussed. In Section III, the architecture of the optimal receiver is derived, and its error probability bounds are obtained and compared with that of the Genie-aided receiver. A sub-optimal receiver, the equal-gain-combining receiver, is developed in Section IV, and its performance is compared to that of the Genie-aided receiver.

II. STRUCTURED RECEIVER ARCHITECTURE

We can design optical receivers using two different approaches. Due to the quantum nature of weak optical signals, one method is to use a full quantum description of the receiver and optimize it over the class of physically realizable measurements [8]. In this paper, we take a second “structured” or “semi-classical” receiver approach [9]. Although they suffer a loss of 3-dB energy efficiency over optimal quantum receivers for binary signaling, they are easy to implement with current techniques. As illustrated in Fig. 2, the architecture of

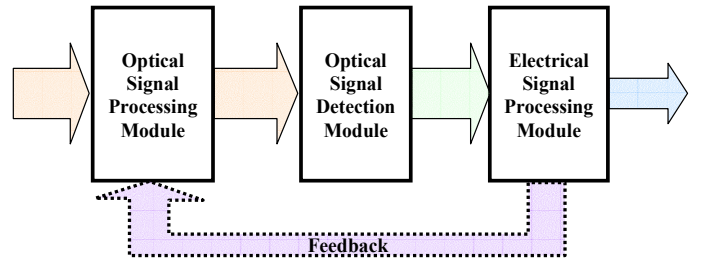


Fig. 2. Structured receiver architecture. It is divided into three cascaded modules: an optical signal processing module, an optical detection module and an electrical signal processing module.

all possible structured receivers can be divided into three cascaded processing modules: an optical signal processing module, an optical detection module, and an electrical signal processing module. The three modules must be jointly optimized to achieve a globally optimal performance. Causal feedbacks among these blocks are also permissible, which can yield structured receivers that achieve the quantum limit for binary signaling [16]. However, due to their complexity, we will not consider them here.

Within the class of structured receivers, the art of practical design is basically a trade-off between implementation complexity and symbol error probability. In general, in order to achieve a lower error probability, the receiver needs to estimate the lightpath states for symbol decisions. This joint estimation and detection approach can result in a complicated receiver structure. On the other hand, a simpler receiver uses simpler lightpath state estimators or does not estimate the lightpath states at all, but usually has a higher error probability since it does not exploit all the information available at the receiver. In this paper, we explore two extreme cases for the complexity-error trade-off:

1) *The optimal receiver*: It has the lowest symbol error probability, but has the most complicated receiver architecture.

2) *The Equal-Gain-Combining receiver*: The receiver architecture is much simpler. However, the error performance is sub-optimum since it does not exploit all the available information at the receiver.

Between the two extreme cases are other reasonably good sub-optimal receivers. Their error performance is usually better than that of the equal-gain-combining receiver, and worse than that of the optimal receiver. On the other hand, their complexity is higher than that of the equal-gain-combining receiver, and lower than that of the optimal receiver. One of our objectives in this research is to understand how these receivers perform in different SNR regimes and generalize rules of thumb to balance the complexity-error trade-off in practical optical receiver design.

III. OPTIMUM RECEIVER

In this section, we seek the optimal receiver that can be implemented with current optical and electronic techniques. In particular, at the optical signal processing module, optical delay lines are used to compensate for delay variations among different lightpaths (fiber delays can also be replaced by time delays in the electrical processing stage since we will use M parallel detectors); at the detection module, photon-counting receivers are used to record the photo-event time statistics for symbol decisions; at the electrical processing module, we use a Maximum Likelihood (ML) detector to make symbol decisions based on the recorded photo-event time statistics.

A. System Model

We assume that the physical topology of an all-optical network has dense enough connections such that M independent lightpaths can always be found between source-destination pair [14][15]. Physically, all the lightpaths must belong to different shared-risk groups to avoid correlated failures. Each lightpath is modeled as an additive-noise channel with UP and DOWN states [6], as shown in Fig. 1. In particular, the input-output relation is given by $Y = FX + N$, where X and Y are the input signal and the output signal, F is the lightpath state indicator function which is a Bernoulli random variable with $\Pr(F = 0) = f$ and $\Pr(F = 1) = 1 - f$, and N is the additive noise (zero if no optical amplifier is used). For a given source-destination pair, we define $\mathbf{F} = (F_1, F_2, \dots, F_M)^T$ as the lightpath state vector, where F_i 's are identically and independently distributed Bernoulli random variables.

Binary Pulse-Position Modulation (BPPM) is used to simplify the receiver implementation by not having to adaptively set the decision threshold as in the case of On-Off-Keying (OOK). The modulated signal is split into M parts. Each part is sent through an independent lightpath to the receiver. Under the assumption of homogenous lightpaths, i.e., the lightpath state indicator functions and the noises are the same for all the lightpaths, a uniform power allocation algorithm is optimal [6]. At the destination node, the receiver combines optical signals received over M disjoint lightpaths to make symbol-by-symbol decisions.

With direct detection, the photo-event process obeys Poisson statistics [10] if the optical signal is generated by a single-mode laser, which is usually the case for high-speed optical networks. The photo-event rate λ (the photo-event count per unit time) is determined by the received optical power (energy per bit). In our case, the received optical power is a random variable due to the random channel model. It follows that the photo-event process at the detector output can be modeled as a Doubly-Stochastic Point Process [7].

B. Receiver Architecture

Because uniform power allocation is employed at the transmitter, the optical power transmitted over the i^{th} lightpath is either

$$P_i^{(0)}(t) = \begin{cases} P_s/M & 0 \leq t \leq T/2 \\ 0 & T/2 \leq t \leq T \end{cases} \quad (1)$$

for hypothesis H_0 (i.e., symbol "0"), or

$$P_i^{(1)}(t) = \begin{cases} 0 & 0 \leq t \leq T/2 \\ P_s/M & T/2 \leq t \leq T \end{cases} \quad (2)$$

for hypothesis H_1 (i.e., symbol "1"). In both cases, P_s is the average output power of the laser, and T is the symbol time.

The received optical signals can be corrupted by amplifier noises if optical amplifiers are used. We assume that the noise process receives contributions from many spatial-temporal modes, and the probability of two successive noise-driven photo-events coming from the same spatial-temporal mode is close to zero. It follows that the Weak Photon-Coherence Assumption holds, and thus we can approximate the noise-driven photo-event process with a Poisson Process with a deterministic rate of λ_n equal to its mean. Consequently, considering the noise, the photo-event rate at the output of the i^{th} detector is either

$$\lambda_i^{(0)}(t) = \begin{cases} F_i \lambda_s / M + \lambda_n & 0 \leq t \leq T/2 \\ \lambda_n & T/2 \leq t \leq T \end{cases} \quad (3)$$

for hypothesis H_0 , or

$$\lambda_i^{(1)}(t) = \begin{cases} \lambda_n & 0 \leq t \leq T/2 \\ F_i \lambda_s / M + \lambda_n & T/2 \leq t \leq T \end{cases} \quad (4)$$

for hypothesis H_1 . In both cases, $\lambda_s = \eta P_s / h\nu$ (η is the photo efficiency, $h\nu$ is the photon energy) is the rate of a photo-event process with an average power P_s , and F_i is a Bernoulli random variable with parameter $1 - f$. Note that, for a given hypothesis, the photo-event process is a Doubly-Stochastic Point Process due to its random rate.

For the i^{th} channel, let (k_{i1}, k_{i2}) be the photo-event counts during $[0, T/2]$ and $[T/2, T]$, and $(\mathbf{t}_{i1}, \mathbf{t}_{i2}) = (t_1, t_2, \dots, t_{k_{i1}}, t_{k_{i1}+1}, t_{k_{i1}+2}, \dots, t_{k_{i1}+k_{i2}})$ be the corresponding photo-event time statistics. The conditional distribution density functions of time statistics at the i^{th} lightpath, as derived in [7][13], are given by

$$p(\mathbf{t}_{i1}, \mathbf{t}_{i2} | H_0) = \left[\prod_{j=1}^{k_{i1}} \left(\widehat{F}_i^{(0)}(t_j) \frac{\lambda_s}{M} + \lambda_n \right) \right] (\lambda_n)^{k_{i2}} e^{-\frac{\lambda_s}{M} \int_0^{T/2} \widehat{F}_i^{(0)}(t) dt - 2N_n} \quad (5a)$$

and

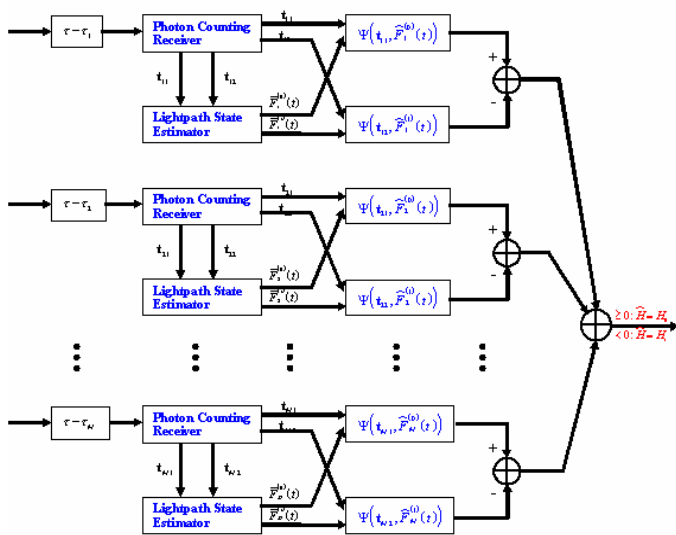


Fig. 3. Optimal receiver architecture.

$$\Psi_1(\mathbf{t}_{i1}, \hat{F}_i^{(0)}(t)) = \sum_{j=1}^{k_{i1}} \ln(1 + \hat{F}_i^{(0)}(t_j)\Omega) - \frac{\lambda_s}{M} \int_0^{T/2} \hat{F}_i^{(0)}(t) dt \quad \text{where } \mathbf{t}_{i1}$$

are photo-event time statistics and $\hat{F}_i^{(0)}(t)$ are channel state estimators under H_0 .

$$\Psi_2(\mathbf{t}_{i2}, \hat{F}_i^{(1)}(t)) = \sum_{j=1}^{k_{i2}} \ln(1 + \hat{F}_i^{(1)}(t_{j+k_{i1}})\Omega) - \frac{\lambda_s}{M} \int_{T/2}^T \hat{F}_i^{(1)}(t) dt \quad \text{where } \mathbf{t}_{i2}$$

are photo-event time statistics and $\hat{F}_i^{(1)}(t)$ are channel state estimators under H_1 .

$$p(\mathbf{t}_{i1}, \mathbf{t}_{i2} | H_1) = (\lambda_n)^{k_{i1}} \left[\prod_{j=1}^{k_{i2}} \left(\hat{F}_i^{(1)}(t_{j+k_{i1}}) \frac{\lambda_s}{M} + \lambda_n \right) \right] e^{-\frac{\lambda_s}{M} \int_{T/2}^T \hat{F}_i^{(1)}(t) dt - 2N_i} \quad (5b)$$

where

$$\hat{F}_i^{(j)}(t) = \begin{cases} E[F_i^{(j)} | H_j, N_i = 0] & N_i = 0 \\ E[F_i^{(j)} | H_j, N_i = k, \mathbf{t}_{i1}, \mathbf{t}_{i2}] & N_i = k \geq 1 \end{cases} \quad (6)$$

is the minimum mean squared error (MMSE) causal estimator of the i^{th} lightpath state for hypotheses H_j ($j=0,1$) and N_i is photo-event count over $[0, t]$. As derived in *Appendix A*, these estimators are given by

$$\hat{F}_i^{(0)}(t) = \frac{1}{1 + \frac{f}{1-f} \exp\left(\frac{\lambda_s}{M} t\right) (1+\Omega)^{-N_i}} \quad t \in \left[0, \frac{T}{2}\right], \quad (7)$$

where N_i is the photo-event count over $[0, t]$, and

$$\hat{F}_i^{(1)}(t) = \frac{1}{1 + \frac{f}{1-f} e^{\frac{\lambda_s}{M} (t - \frac{T}{2})} (1+\Omega)^{-(N_i - N_{i2})}} \quad t \in \left[\frac{T}{2}, T\right], \quad (8)$$

where N_i is the photo-event count over $[0, t]$, and N_{i2} is the photo-event count over $[0, T/2]$ of the same realization of the photo-event process. The fact that both estimators described in (7) and (8) depend only causally on the recorded photo-event counts, suggests that the detector can be updated continuously in real time as the doubly stochastic point process is being observed. This property allows two important realizations of the optimal receiver. The first one is that real-time receiver processing can be used for delay sensitive traffic. The second one is that the sequential hypothesis testing reduces the error probability further by making symbol decisions based on the photo-event statistics over several consecutive previous data bits.

Note that photo-event processes of different lightpaths are independent because each lightpath belongs to a different shared-risk group. It follows that the overall conditional distribution density function can be written as

$$p(\mathbf{t}_1, \mathbf{t}_2 | H_0) = \prod_{i=1}^M p(\mathbf{t}_{i1}, \mathbf{t}_{i2} | H_0) \quad (9a)$$

and

$$p(\mathbf{t}_1, \mathbf{t}_2 | H_1) = \prod_{i=1}^M p(\mathbf{t}_{i1}, \mathbf{t}_{i2} | H_1), \quad (9b)$$

where $(\mathbf{t}_1, \mathbf{t}_2) = (\mathbf{t}_{11}, \mathbf{t}_{21}, \dots, \mathbf{t}_{M1}, \mathbf{t}_{12}, \mathbf{t}_{22}, \dots, \mathbf{t}_{M2})$ is the overall photo-event time statistics. Using (9a) and (9b), the log likelihood-ratio can be written as

$$\ln \Lambda\{\mathbf{t}, \mathbf{N}_1, \mathbf{N}_2 : 0 \leq t \leq T\} = \ln \frac{p(\mathbf{t}_1, \mathbf{t}_2, \mathbf{N}_1, \mathbf{N}_2 | H_0)}{p(\mathbf{t}_1, \mathbf{t}_2, \mathbf{N}_1, \mathbf{N}_2 | H_1)} = \sum_{i=1}^M \left[\sum_{j=1}^{k_{i1}} \ln(1 + \hat{F}_i^{(0)}(t_j)\Omega) - \frac{\lambda_s}{M} \int_0^{T/2} \hat{F}_i^{(0)}(t) dt \right] - \sum_{i=1}^M \left[\sum_{j=1}^{k_{i2}} \ln(1 + \hat{F}_i^{(1)}(t_{j+k_{i1}})\Omega) - \frac{\lambda_s}{M} \int_{T/2}^T \hat{F}_i^{(1)}(t) dt \right] \quad (10)$$

where $\Omega = \lambda_s / M \lambda_n$ can be interpreted as the signal-to-noise ratio per lightpath. After some algebraic manipulations, we obtain the maximum likelihood detection rule as

$$\sum_{i=1}^M \left\{ \sum_{j=1}^{k_{i1}} \ln(1 + \hat{F}_i^{(0)}(t_j)\Omega) - \frac{\lambda_s}{M} \int_0^{T/2} \hat{F}_i^{(0)}(t) dt \right\} \stackrel{\hat{H}=H_0}{\geq} \sum_{i=1}^M \left\{ \sum_{j=1}^{k_{i2}} \ln(1 + \hat{F}_i^{(1)}(t_{j+k_{i1}})\Omega) - \frac{\lambda_s}{M} \int_{T/2}^T \hat{F}_i^{(1)}(t) dt \right\} \stackrel{\hat{H}=H_1}{<} \quad (11)$$

Note that each received photon is weighed by the scaling factor of $\ln(1 + \hat{F}_i(t_j)\Omega)$ which depends on the lightpath state estimate at the photon arrival time. If the estimate of the lightpath state is large meaning that the possibility of the lightpath being UP is high, the scaling factor is large since it is more likely that the photon comes from the signal, not noise. On the contrary, we assign a small scaling factor to the photon

if the lightpath state estimate is small. In particular, if we estimate that the lightpath is DOWN, the scaling factor is equal to zero since the photon must come from noise and thus could not be taken into consideration for detection.

For a sanity check, assuming all the lightpaths are ON(i.e., $\widehat{F}_i^{(0)}(t) = \widehat{F}_i^{(1)}(t) = 1$) during the symbol transmission, Decision rule (11) simplifies to be

$$\sum_{i=1}^M k_{i1} \underset{\widehat{H}=H_1}{\geq} \sum_{i=1}^M k_{i2} \quad (12)$$

Detection rule (12) is identical to the detection rule for the case with invulnerable lightpaths [11]. Detection rule (11) indicates a fundamental decomposition of functions in the optimal receiver structure, which is generalized as the separation theorem of detection in [7]. In particular, the receiver consists of two separable operation modules, i.e., estimators for lightpath states and signal processing modules for hypothesis testing, as shown in Fig. 3. This separation property suggests that we can replace the complicated optimal lightpath state estimator with some simpler heuristic state estimators to reduce the receiver complexity without modifying the receiver structure. This idea often performs well in practice and yields near-optimal policies in dynamic programming [17]. Therefore, we expect that the error performance with sub-optimal lightpath state estimators is not degraded significantly, which indeed is true, as will be shown in next section.

C. Error Performance

In this subsection, we analyze the error performance of the optimal receiver. In particular, a lower bound and an upper bound are derived for the Chernoff Bound of the symbol error probability.

As illustrated in [6], the symbol error probability of the genie-aided receiver is the Genie-aided limit of the proposed architecture within the class of structured receivers. For a sense of how best the optimal receiver could perform, we can use the Chernoff Bound of the genie-aided receiver as a lower bound for Chernoff Bound of the optimal receiver because the Chernoff Bound is exponentially tight [12]. This suggests that a natural lower bound for the Chernoff error bound of the optimal receiver,

$$PB_{opt} \geq \left[f + (1-f)e^{-\psi(N_s, N_n, M)} \right]^M \triangleq PB_{opt}^{LB}, \quad (13)$$

where $\psi(N_s, N_n, M) = \left(\sqrt{N_s/M + N_n} - \sqrt{N_n} \right)^2$, $N_s = \lambda_s T/2$ is the average number of signal-driven photo-events per bit, $N_n = \lambda_n T/2$ is the average number of noise-driven photo-events per half a bit, and PB_{opt} is the error bound of the optimal receiver.

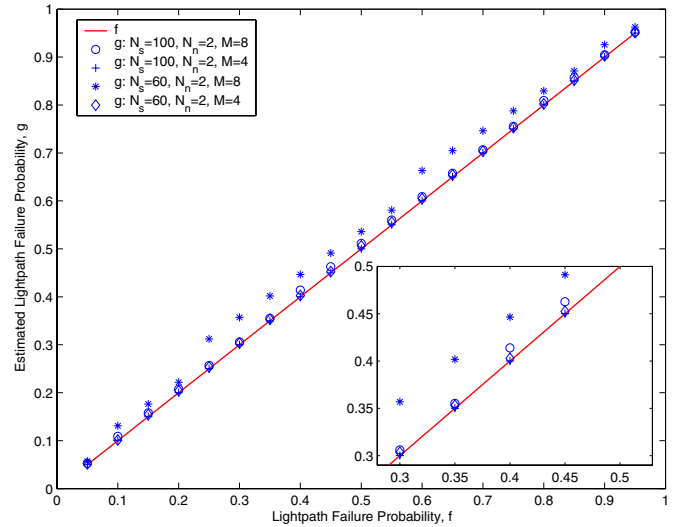


Fig. 4. The estimated lightpath failure probability g is compared to the prior lightpath failure probability f under different SNRs per lightpath.

On the other hand, the optimal receiver must perform better than any suboptimal receiver within the class of structured receivers [13]. It follows that we can use the Chernoff Bound of any suboptimal receiver as an upper error bound for the optimal receiver. In particular, we choose a suboptimal receiver that estimates UP/DOWN states of all the lightpaths at time $t = T$. An intuitive estimation rule is

$$\begin{aligned} \text{if } \widehat{F}(T) \leq 0.5 & \quad \widetilde{F} = 0 \\ \text{if } \widehat{F}(T) > 0.5 & \quad \widetilde{F} = 1 \end{aligned} \quad (14)$$

where $\widehat{F}(T)$ is the MMSE causal estimate of the channel state at time $t = T$ and \widetilde{F} is the estimated lightpath state. If $\widetilde{F} = 0$, the receiver estimates the lightpath to be DOWN and thus discards the received signal over that lightpath. Otherwise, the receiver estimates the lightpath to be UP and thus uses the received optical signal over that lightpath for optimal combining and symbol decisions.

As derived in *Appendix B*, the upper bound for the Chernoff error bound of the optimal receiver, which is also the Chernoff error bound of the suboptimal receiver, is given by

$$PB_{opt} \leq \left[g + (1-g)e^{-\psi(N_s, N_n, M)} \right]^M \triangleq PB_{opt}^{UP}. \quad (15)$$

Here, the probability that the lightpath is estimated to be DOWN, $g = \Pr(\widehat{F}(T) \leq 1/2)$, is given by

$$g = f \sum_{k=0}^{N_{TH}} \frac{(N_n)^k}{k!} e^{-N_n} + (1-f) \sum_{k=0}^{N_{TH}} \frac{\binom{N_s}{M} + N_n}{k!} e^{-\left(\frac{N_s}{M} + N_n\right)}. \quad (16)$$

where

$$N_{TH} = \frac{N_s/M + \ln(f/(1-f))}{\ln(1 + N_s/MN_n)} \quad (17)$$

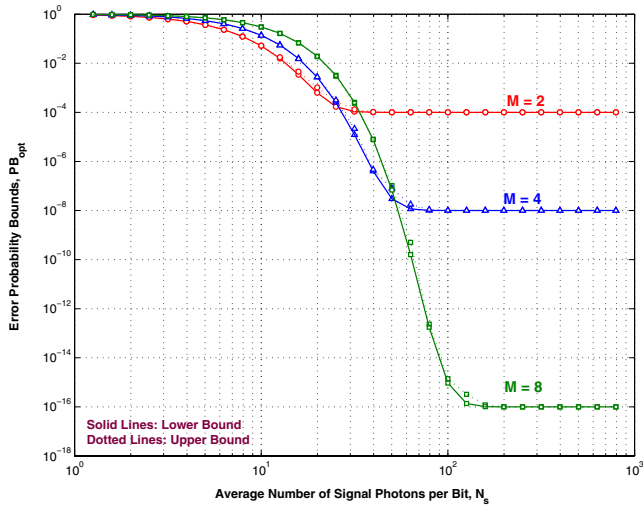


Fig. 5. The lower bound and the upper bound for the Chernoff bound of the optimal receiver. The number of lightpaths is set as $M = 2, 4, 8$, and lightpath failure probability is 0.01, the noise level per lightpath is 2.

is the number of photons per bit beyond which the lightpath is estimated to be UP. In (17), N_s/M is the average number of photons per lightpath per bit, $\ln[f/(1-f)]$ is the additional number of photons needed to declare that the lightpath is UP, and both numbers must be adjusted by the term $\ln(1+N_s/MN_n)$ that is the scaling factor in (11) to obtain the actual number of photons. If $0 < f < 1/2$, then $\ln[f/(1-f)] < 0$. This means that the actual number of photons needed is reduced since the probability of the lightpath being UP is higher and fewer photons per lightpath are needed for the estimator to declare that the lightpath is UP. On the other hand, if $1/2 < f < 1$, then $\ln[f/(1-f)] > 0$. This means that the actual number of photons needed is increased since the probability of the lightpath being DOWN is higher and more photons per lightpath are needed for the estimator to declare that the lightpath is UP.

Note that the lower bound (13) and the upper bound (15) have the same form, except that the prior lightpath failure probability f in (13) is replaced by the estimated lightpath failure probability g in (16). This implies that the tightness of the lower bound and the upper bound highly depends on the difference between the estimated lightpath failure probability and the prior lightpath failure probability. To explore this, we compare the estimated lightpath failure probability g with the prior failure probability f in Fig. 4. We find that the difference between these two probabilities is negligible when the SNR per lightpath is high enough. It follows that the lower bound and the upper bound are close to each other, and thus both are very tight. This is verified in Fig. 5 where the lower bound and the upper bound are plotted against the average number of photons per bit. Moreover, these tight bounds suggest that the optimal

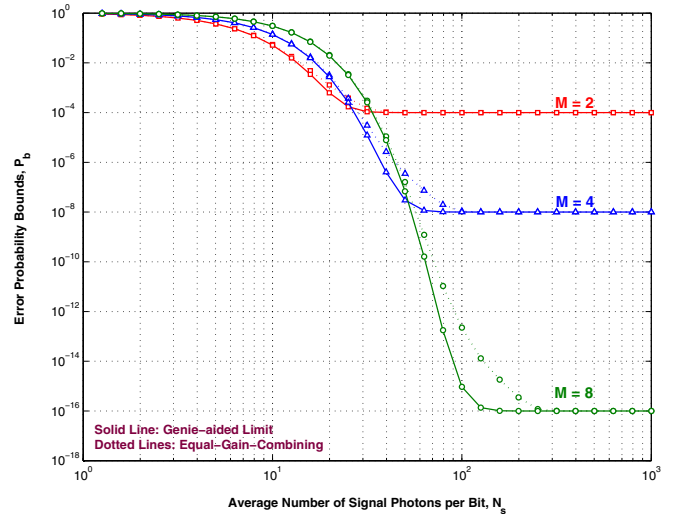


Fig. 6. Error bounds of the equal-gain-combining receiver are compared with the ‘genie-aided’ receiver limit under different lightpath numbers. ($f = 0.01$, $N_n = 2$.) Limit: the fundamental limit; EGC: equal-gain-combining receiver.

receiver exhibits the same error characteristics in different SNR regimes as the ‘genie-aided’ receiver, as shown in Fig. 5. In the super-high SNR regime, the error bound converges to an error floor f^M , the probability with which the source-destination pair is disconnected. This suggests that network topologies with small probability of disconnection [14][15] should be considered for ultra-high reliable optical networks. In the lower SNR regime, the error probability increases with more lightpaths. It indicates that lightpath diversity actually hurts in this regime and be of no engineering interest. In the medium-to-high SNR regime, the error probability depends on both the number of lightpaths and the SNR per lightpath. These two factors, however, are competing with each other for a given amount of optical energy. Hence, we need to balance this trade-off to achieve better energy efficiency. This, along with the fact that the optimal receiver performs close to the ‘genie-aided’ receiver limit, suggests that system parameters optimized for the genie-aided receiver, such as the optimum number of lightpaths derived for different objective functions [6], also apply for the optimal receiver in the medium-to-high SNR regime.

IV. EQUAL-GAIN-COMBINING RECEIVER

Although the optimal receiver has the lowest symbol error probability, it requires the most complicated processing by estimating the individual lightpath state throughout the symbol time. In this section, we develop one sub-optimal receiver, the equal-gain-combining receiver, which not only approaches the optimal receiver in the symbol error probability under some scenarios, but also has the advantage of a simpler architecture.

A. Receiver Architecture

In the equal-gain-combining receiver, rather than estimate lightpath states, we assume all the lightpaths to be UP and use the Maximum Likelihood decision rule to do symbol detection. Mathematically, the equal-gain-combining receiver employs the following decision rule

$$\sum_{i=1}^M k_{i1} \underset{\hat{H}=H_1}{\geq} \sum_{i=1}^M k_{i2} \quad (18)$$

to make symbol-to-symbol decision based only on the photo-event counts. Decision rule (18) is much simpler than decision rule (11). This indicates that the equal-gain-combining receiver offer a significant reduction in the implementation complexity compared to the optimal receiver. However, the reduction in complexity is traded with a degraded error performance, as shown in the following subsection.

B. Error Performance

We start with the calculation of the error bound for the equal-gain-combining receiver. Given the lightpath state vector \mathbf{F} , the conditional error probability is defined by

$$\begin{aligned} \Pr(\mathcal{E} | \mathbf{F}) &= p_0 \Pr \left[\sum_{i=1}^M k_{i1} \leq \sum_{i=1}^M k_{i2} \mid H_0, \mathbf{F} \right] \\ &\quad + p_1 \Pr \left[\sum_{i=1}^M k_{i1} \geq \sum_{i=1}^M k_{i2} \mid H_1, \mathbf{F} \right], \quad (19) \\ &= \Pr \left[\sum_{i=1}^M k_{i1} \leq \sum_{i=1}^M k_{i2} \mid H_0, \mathbf{F} \right] \end{aligned}$$

where p_0, p_1 are probabilities of sending the ‘‘ZERO’’ or ‘‘ONE’’ bit, and the second equality is due to the symmetry of binary pulse-position modulation and $p_0 = p_1 = 1/2$ for equiprobable digital source.

Let $K_1 = \sum_{i=1}^M k_{i1}$ be the total photo-event count recorded over $[0, T/2]$, and $K_2 = \sum_{i=1}^M k_{i2}$ be the total photo-event count recorded over $[T/2, T]$. Note that, given hypothesis H_0 and the lightpath state vector \mathbf{F} , K_1 is a Poisson random variable with mean $mN_s/M + MN_n$ where $m = \sum_{i=1}^M F_i$ is the number of UP lightpaths for a given lightpath state vector \mathbf{F} , and K_2 is a Poisson random variable with mean MN_n .

Using the Chernoff Bound, the conditional error probability is bounded by

$$\Pr(\mathcal{E} | \mathbf{F}) \leq \exp \left\{ - \left(\sqrt{\frac{N_s}{M} m + MN_n} - \sqrt{MN_n} \right)^2 \right\}. \quad (20)$$

It can be verified that m is a binominal random variable with a distribution function of $\Pr\{m = k\} = \binom{M}{k} (1-f)^k f^{M-k}$, $k = 0, 1, \dots, M$. Averaging (20) over all possible lightpath state vectors $\mathbf{F} \in \{0, 1\}^M$, we obtain the error bound for the equal-gain-combining receiver as

$$\Pr(\mathcal{E}) \leq \sum_{k=0}^M \frac{M!}{k!(M-k)!} (1-f)^k f^{M-k} e^{-\left(\sqrt{\frac{N_s}{M} k + MN_n} - \sqrt{MN_n} \right)^2}. \quad (21)$$

Using (21), we compare the error bound of the equal-gain-combining receiver with the ‘genie-aided’ receiver limit in Fig. 6. In the low SNR regime, the error probability is inherently high and of no engineering interest. In the medium-to-high SNR regime, the gap between error bounds of the equal-gain-combining receiver and the ‘genie-aided’ limit is larger than the gap between error bounds of the optimal receiver and the ‘genie-aided’ limit. In the equal-gain-combining receiver, noise from DOWN lightpaths will degrade the average SNR per lightpath and thus increases the error probability since the error probability in the medium-to-high SNR regime is sensitive to the SNR per lightpath. However, in the high SNR regime, the equal-gain-combining receiver has an error bound close to the ‘genie-aided’ receiver limit. This indicates that the equal-gain-combining receiver is preferable to the optimal receiver in the high SNR regime due to its simplicity. In fact, the equal-gain-combining receiver approaches asymptotically the optimal receiver when the noise is negligible, as we will show next.

C. Power Penalty

Since the error probability of the equal-gain-combining receiver is higher than that of the ‘genie-aided’ receiver, we need to transmit more optical energy in order for the equal-gain-combining receiver to achieve the same target error probability as the ‘genie-aided’ receiver does in the medium-to-high SNR regime. In this subsection, we analyze this amount of additional power for the equal-gain-combining receiver to achieve a target error probability bound compared to the genie-aided receiver. For a target error probability bound of P_b , the power penalty of the equal-gain-combining receiver over the ‘genie-aided’ receiver is defined as

$$\delta = 10 \log_{10} \left(\frac{N_s^*(P_b, f, N_n; EGC)}{N_s^*(P_b, f, N_n; GA)} \right), \quad (22)$$

where $N_s^*(P_b, f, N_n; GA)$ and $N_s^*(P_b, f, N_n; EGC)$ are the minimum amounts of optical power (in terms of average number of signal photons per bit) for the genie-aided receiver and the equal-gain-combining receiver respectively to achieve a target error probability P_b .

Using numerical results by exhaustive searching, the optimal number of lightpaths and the minimum transmitted

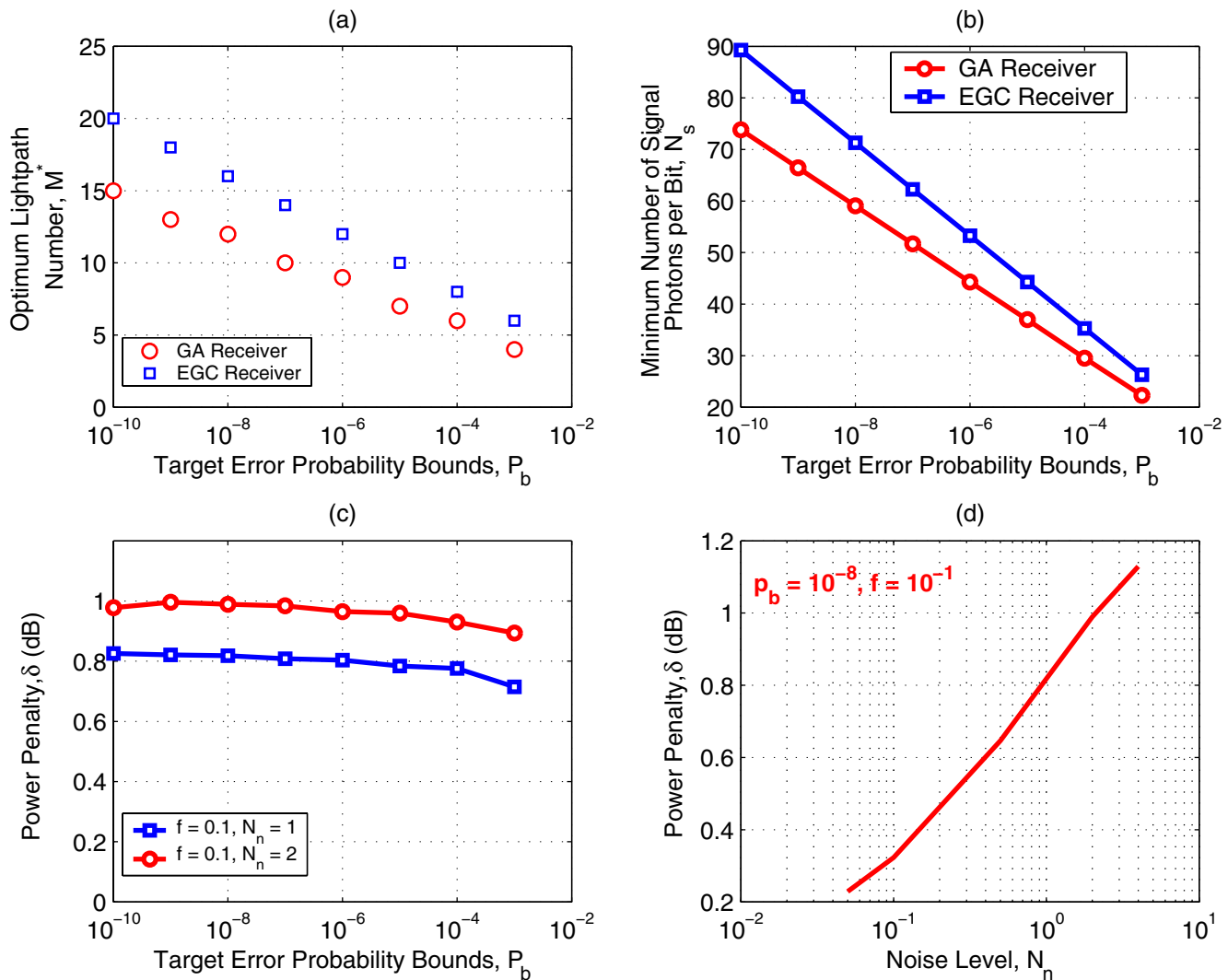


Fig. 7. (a) The optimal lightpath number to minimize the total optical energy is plotted against different target error probability bounds. (b) The minimum number of signal photons per bit is plotted against different target error probability bounds for the ‘genie-aided’ receiver and the equal-gain-combining receiver. In plot (a) and (b), we set $f = 0.1$ and $N_n = 2$. GA: Genie-aided receiver; EGC: Equal-gain-combining receiver. (c) Power penalty of the equal-gain-combining receiver is plotted under different target error probability bounds. (d) Power penalty of the equal-gain-combining receiver is plotted under different noise levels.

optical energy are plotted in Fig. 7 (a) and (b). To achieve the same error probability bound, the equal-gain-combining receiver requires more lightpaths to be used and more optical energy to be transmitted. This shows that a more densely-connected network topology is needed to provide enough independent lightpaths for the equal-gain-combining receiver. The power penalty is plotted in Fig. 7 (c) and (d). From plot (c), the power penalty is asymptotically invariant of the target error probability bounds. This is due to two reasons. First, the error bound of the equal-gain-combining receiver is close to that of the genie-aided receiver with optimized system parameters. Second, the minimum transmitted power is linear with the error exponent (see (10) in [6]). It follows that, at the optimum operating points, both error bounds are parallel to each other in a log-log plot. The power penalty is approximately determined by the ratio between the slopes of

the error exponents of the ‘genie-aided’ receiver and the equal-gain-combining receiver at the respective optimum operating points. Therefore, the power penalty is invariant with respect to target error probabilities. On the other hand, the power penalty increases with higher noise levels as shown in plot (d), and approaches zero when the noise level goes to zero. This demonstrates that the equal-gain-combining receiver is generally suboptimal and approaches the optimal receiver when the noise level decreases. In particular, if there is no noise, the equal-gain-combining receiver would be optimal under the maximum likelihood criterion because the receiver would not receive any noise from DOWN lightpaths to degrade the error performance.

V. CONCLUSION

In this paper, we investigated a class of structured receivers for the multiple-lightpath transmission scheme in vulnerable optical networks. Using a Doubly-Stochastic Point Process model, we developed the architecture of the optimal receiver, and calculated its error performance with a lower bound (the genie-aided receiver) and an upper bound (the noncausal-state-estimating receiver). The small gap between the lower bound and the upper bound indicates that the optimal receiver approaches the Genie-aided limit of structured receivers, and thus system parameters optimized for the genie-aided receiver apply to the optimal receiver. However, the optimal receiver needs to estimate lightpath states throughout the symbol time, which is complicated. To balance the trade-off between the error probability and the implementation complexity, we developed the simplest suboptimal receiver, i.e., the equal-gain-combining receiver, and characterized its error performance. The performance comparison between the equal-gain-combining receiver and the Genie-aided limit of structured receivers shows that the power penalty of the equal-gain-combining receiver decreases with decreasing noise levels. These results suggest that the equal-gain-combining receiver is preferable to the optimal receiver in the low noise regime, and the optimal receiver is needed in the high noise regime at the expense of increased complexity.

APPENDICES

A. MMSE Lightpath State Estimator for Optimum Receiver

In designing the optimal receiver, we need to find the MMSE causal estimator of lightpath states. We start by incorporating the following lemma in [7], which is crucial to the derivation of the MMSE causal lightpath state estimator.

Lemma 1 (*Estimation of random variables in Doubly Stochastic Point Processes*): For a Doubly Stochastic Point-Process $\{N(t): t \geq t_0\}$ with a random arrival rate $\lambda(t, \mathbf{x})$, where \mathbf{x} is a time-independent random vector, let $\mathbf{a}_t(\mathbf{x})$ be a time-dependent vector-value function of the random vector \mathbf{x} and such that $E\left(\|\mathbf{a}_t(\mathbf{x})\|^2\right) < \infty$. Then, for a recorded time statistic $\{\mathbf{t} = (t_1, t_2, \dots, t_n)\}$, the MMSE causal estimate of the function $\mathbf{a}_t(\mathbf{x})$ of \mathbf{x} is the conditional mean $\hat{\mathbf{a}}_t$, given by

$$\hat{\mathbf{a}}_t = E\left[\mathbf{a}_t(\mathbf{x}) \mid \mathbf{t} = (t_1, t_2, \dots, t_n)\right] = \frac{E\left\{\mathbf{a}_t(\mathbf{x}) \exp\left[\mathbf{A}_t(\mathbf{x})\right]\right\}}{E\left\{\exp\left[\mathbf{A}_t(\mathbf{x})\right]\right\}}, \quad (\text{A.1})$$

where $\mathbf{A}_t(\mathbf{x}) = -\int_{t_0}^t \lambda(\tau, \mathbf{x}) d\tau + \int_{t_0}^t \ln \lambda(\tau, \mathbf{x}) dN_\tau$. \square

For simplicity, the subscript i is suppressed in the following derivation. Due to the random channel model, the arrival rate of the photo-event process at the output of each detector, $\lambda(t, F) = F\lambda(t) + \lambda_n$, is a random variable. In

particular, F is a Bernoulli random variable with the probability density function $p_F(x) = f\delta(x) + (1-f)\delta(x-1)$.

Using (C.1), the MMSE causal estimator of the channel state F is given by

$$\hat{F}(t) = E[F \mid \mathbf{t}] = \frac{E\left\{F \exp\left[A_t(F)\right]\right\}}{E\left\{\exp\left[A_t(F)\right]\right\}}, \quad (\text{A.2})$$

where $A_t(F) = -\int_0^t \lambda(\tau, F) d\tau + \int_0^t \ln \lambda(\tau, F) dN_\tau$.

For hypothesis H_0 , the photo-event rate is

$$\lambda^{(0)}(t) = \begin{cases} F\lambda_s/M + \lambda_n & 0 \leq t \leq T/2 \\ \lambda_n & T/2 \leq t \leq T \end{cases} \quad (\text{A.3})$$

Substituting (A.3) into (A.2), the MMSE causal estimator of the channel state F turns out to be

$$\hat{F}^{(0)}(t) = \frac{1}{1 + \frac{f}{1-f} \exp\left(\frac{\lambda_s}{M} t\right) (1+\Omega)^{-N_t}} \quad t \in \left[0, \frac{T}{2}\right]. \quad (\text{A.4})$$

where N_t is the number of photo-events over $[0, t]$.

For hypothesis H_1 , the photo-event rate is

$$\lambda^{(1)}(t) = \begin{cases} \lambda_n & 0 \leq t \leq T/2 \\ F\lambda_s/M + \lambda_n & T/2 \leq t \leq T \end{cases} \quad (\text{A.5})$$

Substituting (A.5) into (A.2), the MMSE causal estimator of the channel state F turns out to be

$$\hat{F}^{(1)}(t) = \frac{1}{1 + \frac{f}{1-f} e^{\frac{\lambda_s}{M}\left(t - \frac{T}{2}\right)} (1+\Omega)^{-(N_t - N_{T/2})}} \quad t \in \left[\frac{T}{2}, T\right]. \quad (\text{C.6})$$

where N_t is the photo-event count over $[0, t]$, and $N_{T/2}$ is the number photo-event count over $[0, T/2]$ of the same sample function of photo-event process.

B. Chernoff Bound of the Symbol Error Probability for the Receiver with Non-causal Lightpath State Estimator

The suboptimal receiver makes hard-decisions on estimated lightpath states from causal state estimators at time $t = T$. The hard-decision rule is given by

$$\begin{aligned} &\text{when } \hat{F}(T) \leq 0.5 \quad \tilde{F} = 0 \\ &\text{when } \hat{F}(T) > 0.5 \quad \tilde{F} = 1 \end{aligned} \quad (\text{B.1})$$

where $\hat{F}(T)$ is the MMSE causal estimate of the lightpath state at time $t = T$. If $\tilde{F} = 0$, the receiver estimates the lightpath to be OFF and thus discards the received signal over that lightpath. Otherwise, the receiver estimates the lightpath to be UP and thus uses the received optical signal over that lightpath for optimal combining and symbol decisions.

With hard-decision lightpath states, the symbol decision rule is given by

$$\sum_{i=1}^m k_{i1} \underset{\hat{H}=H_1}{\geq} \sum_{i=1}^m k_{i2}, \quad (\text{B.2})$$

where m is the number of lightpaths that are estimated to be UP during the symbol transmission. Note that m is a binomial random variable with a probability distribution function,

$$\Pr(m) = \binom{M}{m} (1-g)^m g^{M-m}, \quad (\text{B.3})$$

where $g = \Pr(\hat{F}(T) \leq 0.5)$ is the probability with which the lightpath is estimated to be DOWN during the symbol transmission. For both hypotheses, the channel state estimator has the form,

$$\hat{F} = \left[1 + \frac{f}{1-f} \exp\left(\frac{N_s}{M}\right) (1+\Omega)^{-N} \right]^{-1}. \quad (\text{B.4})$$

The probability distribution function of the photon count is

$$\Pr(N = k) = f \frac{(N_n)^k}{k!} e^{-N_n} + (1-f) \frac{(N_s/M + N_n)^k}{k!} e^{-\left(\frac{N_s}{M} + N_n\right)}. \quad (\text{B.5})$$

Combining (B.4) and (B.5), the probability with which the lightpath is estimated to be DOWN is given by

$$\begin{aligned} g &= \Pr(\hat{F} \leq 0.5) \\ &= \Pr\left(N \leq \frac{N_s/M + \ln(f) - \ln(1-f)}{\ln(1+\Omega)} \triangleq N_{TH}\right) \\ &= \sum_{k=0}^{N_{TH}} \Pr(N = k) \end{aligned} \quad (\text{B.6})$$

To calculate the error bound, we start with the error probability conditioned on the number of lightpaths estimated to be UP during the symbol time. For given m , the conditional error probability is defined as

$$\begin{aligned} \Pr(\mathcal{E} | m) &= p_0 \Pr\left[\sum_{i=1}^m k_{i1} \leq \sum_{i=1}^m k_{i2} \mid H_0, m\right] \\ &\quad + p_1 \Pr\left[\sum_{i=1}^m k_{i1} \geq \sum_{i=1}^m k_{i2} \mid H_1, m\right], \\ &= \Pr\left[\sum_{i=1}^m k_{i1} \leq \sum_{i=1}^m k_{i2} \mid H_0, m\right] \end{aligned} \quad (\text{B.7})$$

where the second equality is due to the symmetry of BPPM. Using the Chernoff Bound, the right hand side of (B.7) is bounded by

$$\begin{aligned} \Pr\left[\sum_{i=1}^m k_{i1} \leq \sum_{i=1}^m k_{i2} \mid H_0, m\right] &\leq \min_{s>0} \left\{ e^{mN_n(e^s-1)} e^{m(N_s/M+N_n)(e^{-s}-1)} \right\} \\ &= \exp\{-m\psi(N_s, N_n, M)\} \end{aligned} \quad (\text{B.8})$$

where $\psi(N_s, N_n, M) = \left(\sqrt{N_s/M + N_n} - \sqrt{N_n}\right)^2$.

Using (B.6) and (B.8), the error bound of the hard-decision receiver is obtained by averaging (B.8) over all possible m , that is,

$$\begin{aligned} \Pr(\mathcal{E}) &= \sum_{m=0}^M \Pr(\mathcal{E} | m) \Pr(m) \\ &\leq \sum_{m=0}^M e^{-m\psi(N_s, N_n, M)} \binom{M}{m} (1-g)^m g^{M-m} \\ &= \left[g + (1-g)e^{-\psi(N_s, N_n, M)} \right]^M \end{aligned} \quad (\text{B.9})$$

Note that (B.9) is also an upper bound for the Chernoff error Bound of the optimal receiver.

REFERENCES

- [1] V. W. S. Chan, et al, "A pre-competitive consortium on wide-band all-optical networks," IEEE/LEOS Journal of Lightwave Technology, Vol. 11, No. 5/6, May/June, 1993, pp. 714-735.
- [2] V. W. S. Chan, "All-Optical Networks," Scientific American 273, No. 3, September 1995, pp. 56-59.
- [3] S. Ramamurthy, and B. Mukherjee, "Survivable WDM Mesh Networks: Part I-Protection," Proceedings of INFOCOM '99, Vol. 2, pp. 744-751, 21-25 Mar 1999.
- [4] S. Ramamurthy, and B. Mukherjee, "Survivable WDM Mesh Networks: Part II- Restoration," ICC '99. Vol.3, pp. 2023-2030, 1999.
- [5] "Architecture of Optical Transport Networks," ITU-T Recommendation G. 872, Feb. 1999.
- [6] Y. G. Wen and V. W. S. Chan, "Ultra-reliable Communication over Unreliable Optical Networks via Lightpath Diversity: Characterization and Optimization," Proceedings of GLOBECOM'2003, San Francisco, December, 2003.
- [7] D. L. Snyder, Random Point Processes, by John Wiley & Sons, Inc., 1975.
- [8] C. W. Helstrom and R. S. Kennedy, "Noncommuting Observables in Quantum Detection and Estimation Theory", IEEE Transaction on Information Theory, Vol. IT-20, No.1, January 1974, pp.16-24.
- [9] S. Karp and J. R. Clark, "Photon Counting: a Problem in Classical Noise Theory", IEEE transaction on information theory, Vol. IT-16, November 1970, pp. 672-680.
- [10] I. Bar-David, "Communication under the Poisson Regime," IEEE Transaction on Information Theory, Vol. IT-15, No. 1, January 1969, pp. 31-37.
- [11] H. L. Van Trees, Detection, Estimation and Modulation Theory, Part I, John Wiley, New York, 1968.
- [12] M. E. Hellman and J. Raviv, "Probability of Error, Equivocation, and the Chernoff Bound," IEEE Transaction on Information Theory, Vol. IT-16, No.4, July 1970, pp. 368-372.
- [13] J. R. Clark, Estimation of Poisson Processes with Applications in Optical Communication, Ph.D. thesis, Dept. of EE, MIT, Cambridge, Mass., September 1971.
- [14] G. Weichenberg, High-Reliability Architectures for Networks under Stress, M.Sc. Thesis, EECS, MIT, 2003.
- [15] G. Weichenberg, Vincent W. S. Chan and Muriel Medard, "High-Reliability Architectures for Networks under Stress," DRCN 2003.
- [16] Samuel Joseph Dolinar, Jr., *A Class of Optical Receivers Using Optical Feedback*, Ph.D. Thesis, MIT, June 1976.
- [17] D. P. Bertsekas, *Dynamic Programming and Optimal Control*, 2nd edition, Athena Scientific, Belmont, Massachusetts, 2000.